

Specific heat of Cr_2O_3 near the Néel temperature*

Richard H. Bruce[†] and David S. Cannell

Department of Physics, University of California at Santa Barbara, Santa Barbara, California 93106

(Received 21 June 1976)

Precise measurements of the specific heat of the uniaxial antiferromagnet Cr_2O_3 near the antiferromagnetic transition temperature are reported. Least-mean-squares analysis of the data yields Heisenberg-like exponents, $\alpha = \alpha' - 0.12$, but the amplitude ratio $A/A' = 0.56$ is not in agreement with experimental results for Heisenberg systems. No indication of crossover to Ising-like behavior near the transition is observed. A critical discussion of the possible effects of systematic error in comparing theoretical and experimental results for the specific heats of magnetic systems is provided.

I. INTRODUCTION

The hypothesis of universality¹ and the results of renormalization-group calculations² indicate that the critical behavior of any system is governed by its dimensionality d and the number of degrees of freedom n of the fluctuations of the order parameter. All systems with given values of d and n supposedly exhibit the same behavior near the critical point, provided the forces are sufficiently short ranged. These ideas have been recently tested for ferromagnetic and antiferromagnetic systems with $d=3$ and $n=3$ by Ahlers and Kornblit,³ who found that the specific heats of those systems for which adequate data were available did exhibit universal behavior in agreement with theory provided allowance was made for the effects of dipolar forces in the ferromagnets. The results obtained in their analysis of the data for each material were, in general, different from the results obtained by the original authors, and in many cases depended on the temperature range for which data were analyzed. For reasons to be presented below, we do not feel this experimental framework to be as rigidly established as is indicated by the errors assigned to various parameters using purely statistical analysis. In fact, we find that when even modest allowances are made for possible systematic errors in the comparison of experiment and theory, the corresponding uncertainties in the parameters become much larger. Viewed in this way the apparent differences between materials belonging to the same universality class, and the dependence of results upon the temperature range analyzed are quite possible, and, in fact, existing data are not seen as capable of providing stringent tests of theoretical results.

We have made precise measurements of the specific heat of Cr_2O_3 in the temperature range $290.68 \leq T \leq 323.43$ K, and have found the antiferro-

magnetic to paramagnetic transition to be very sharp, with no evidence of "rounding" of the specific-heat data for $|t| \equiv |T - T_c|/T_c \geq 2 \times 10^{-4}$. Since Cr_2O_3 is weakly anisotropic, one might expect it to exhibit Heisenberg behavior ($n=3$) with a crossover⁴ to Ising behavior ($n=1$) occurring near T_c . We find no evidence of such crossover in the experimentally accessible temperature range, but the data do not fit naturally into the framework established for pure short-range Heisenberg systems, unless one considers the possibility of systematic effects in comparing data and theory.

In the remainder of this paper we provide a summary of those properties of Cr_2O_3 which are relevant to its critical behavior, describe briefly the novel method used to make the measurements reported here, perform a detailed least-mean-squares analysis of the data, and discuss critically the difficulties involved in extracting reliable information concerning critical behavior from measurements of the specific heat of a magnetic system.

II. PROPERTIES OF Cr_2O_3

Cr_2O_3 exists in the corundum structure with an orthorhombic unit cell.⁵ Below the Néel temperature of ~ 307 K the spins have been studied by neutron scattering,⁶ and are found to align along the c axis, which is the $[111]$ direction of the orthorhombic unit cell. The unit cell with the antiferromagnetic ordering of the spins of the Cr^{3+} ions is shown in Fig. 1. A study of spin waves in Cr_2O_3 at 78 K has been made using inelastic neutron scattering, and has been used to determine exchange constants.⁷ The nearest- and next-nearest-neighbor exchange constants were found to be about 20 times larger than all other exchange constants. The anisotropy field has been determined to be ~ 370 Oe by antiferromagnetic resonance studies.^{7,8} About half this field has been reported to be due to magnetic dipole anisotropy and the

other half to be due to crystalline, or single-ion anisotropy.⁹ The ratio of the anisotropy energy to the exchange energy is $\sim 10^{-4}$, and thus this system might be expected to develop Ising-like behavior ($n=1$), but possibly only very near T_c . X-ray diffraction measurements of the crystal structure of Cr_2O_3 have been made as a function of temperature throughout the transition region.¹⁰ In terms of the hexagonal unit cell the c axis expands at $\sim 5.7 \times 10^{-4}$ Å/K near T_c , while the a dimension expands at the rate of $\sim 3 \times 10^{-5}$ Å/K. The rate of expansion of the c dimension is rather temperature dependent, increasing with increasing temperature, and then abruptly falling to zero at ~ 320 K, which is well above the transition temperature. No indication of any discontinuity in the unit-cell volume was observed at the transition temperature. Measurements of the staggered susceptibility have been made by means of neutron scattering,¹¹ and indicate that the susceptibility diverges as $(T-T_c)^{-1.34 \pm 0.06}$ for $T > T_c$. Measurements of the speed and attenuation of ultrasonic sound have been made as a function of temperature and propagation direction throughout the transition region,¹² and have been interpreted as yielding a specific heat exponent $\alpha = +0.14$ which disagrees with our result $\alpha = -0.12$. The attenuation was observed to diverge strongly as $T \rightarrow T_c$, unlike other magnetic insulators which exhibit rather weak divergences of the attenuation. The effect of hydrostatic pressure upon the unit cell dimensions¹³ and upon the Néel temperature¹⁴ has been studied. Although both the c and a dimensions of the hexagonal unit cell decrease with pressure, the fractional change in a is about 30 times larger than that in c . Despite the fact that c decreases, the effect of pressure is to lower the Néel temperature.

III. METHODS AND RESULTS

The measurements were made using a two-dimensional temperature wave method, which simultaneously measures the specific heat and the thermal conductivity. A detailed description of the method will be provided elsewhere.¹⁵ In essence two thin parallel metal strips deposited on the surface of the sample were used to generate and detect sinusoidal temperature fluctuations. An ac current was passed through one strip which served as a heater, while the other was used as a resistance thermometer. The amplitude of the ac temperature response at the sensing strip can be calculated from the heat diffusion equation using the appropriate boundary conditions, and is given by

$$T_\omega = \frac{P}{\pi \Lambda} \left| \left(\frac{\sinh \frac{1}{2} \alpha w}{\frac{1}{2} \alpha w} \right)^2 K_0(\alpha d) \right|. \quad (1)$$

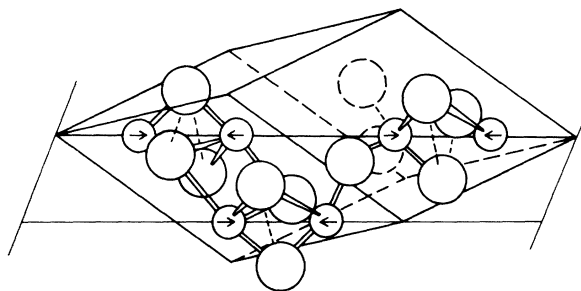


FIG. 1. Structure of Cr_2O_3 . Cr^{3+} ions are distinguished by their spins which are shown in the anti-ferromagnetically ordered state.

Here P is the power per unit length dissipated in the heater, $\alpha = (i\rho c\omega/\Lambda)^{1/2}$, with ρ being the density, c is the specific heat, and Λ is the thermal conductivity of the material, ω is the angular frequency of the ac heating, d is the center-to-center strip separation, w is the strip width, and K_0 is a modified Bessel function of imaginary argument. The specific heat and thermal conductivity were determined by a least-mean-squares fit to Eq. (1) of the ac temperature response measured at eight different heating frequencies ranging from 14 to 680 Hz.

The heating and sensing strips were made by etching a 500-Å thick evaporated nickel film, and were 16 μm wide with a center-to-center spacing of 58.8 μm . The length of the heater was 4.72 mm, and it extended 0.5 mm beyond the ends of the sensor to eliminate end effects. The measurements were made using a single crystal of Cr_2O_3 , $7 \times 5 \times 2$ mm³, grown by the flame fusion technique. Impurities consisted of $\sim 0.1\%$ Al, and 0.1% Mg relative to Cr, and traces of transition-metal ions other than Cr. The measurements were made with the crystal in an environment whose temperature was controlled to within 1 mK. The side of the crystal opposite the strips was in contact with a temperature controlled surface, while the remaining sides were in contact with dry air. The temperature of the sample was measured using a Rosemount Model 146 MA-200 F platinum resistance thermometer. Its resistance was measured using an ac Kelvin Bridge made from two ratio transformers, with a lock-in amplifier as a null detector. The temperature resolution was $\pm 5 \times 10^{-4}$ K, but the absolute temperature was only known to within ± 0.05 K.

The power dissipated in both the heater and sensor was 3 mW/cm. A computer simulation of the temperature distribution due to this heating showed the amplitude of the ac temperature disturbance near the heater to be ~ 30 mK and to be

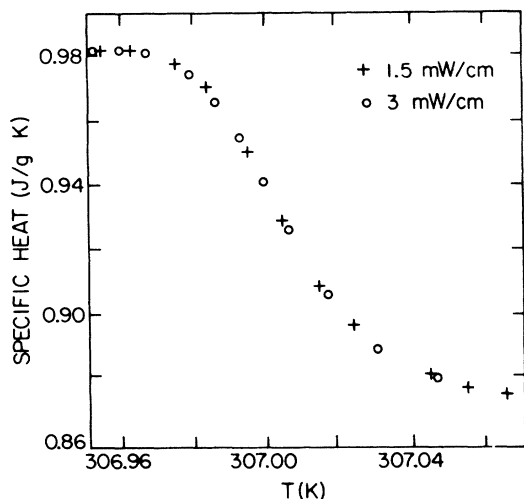


FIG. 2. Specific heat of Cr_2O_3 very near the transition temperature measured using 3 and 1.5 mW/cm heating power. Temperature axis for the results obtained using 1.5 mW/cm has been shifted as discussed in the text.

~ 10 mK near the sensor, at a heating frequency of 14 Hz. In addition the power dissipated in the heater and sensor resulted in a dc temperature difference of ~ 80 mK between the surface of the crystal in the region of the strips and the opposite side, which was in thermal contact with the temperature controller. This dc temperature difference varied $\sim 1\%$ per one degree Kelvin change in the crystal temperature due to the temperature dependence of the thermal conductivity, and it was easy to allow for this small effect. The volume of the sample actually probed by this method lay within ~ 100 μm of the strips, and its dc temperature was uniform to within ± 12 mK when using 3 mW/cm heating power.

In order to determine whether the specific-heat measurements were dependent upon the heating power used, measurements were made near the Néel temperature using powers of 3 and 1.5 mW/cm. The results are shown in Fig. 2, and indicate that the specific-heat measurements are independent of heating power. The temperature axis for the data taken at 1.5 mW/cm has been shifted by ~ 40 mK to allow for the change in the average temperature of the sample volume with heating power. We estimate the specific-heat measurements to be accurate to 2% and they have a precision of 0.1%. In the actual experiment data were taken in two separate runs, each run covering the entire temperature range. The values of the temperature for which data were taken were different for the two runs, but all the results fell on a single smooth curve. The general behavior

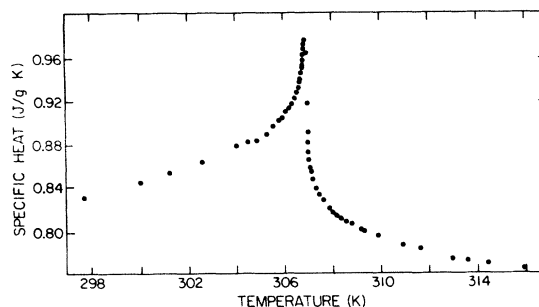


FIG. 3. Specific heat of Cr_2O_3 near the antiferromagnetic transition temperature as a function of temperature.

of the specific heat near the transition may be seen in Fig. 3 which shows most of the data using a linear temperature scale. A more sensitive presentation can be obtained by using a logarithmic temperature scale, and all of the data are displayed this way in Fig. 4. For the sake of accuracy the data are also presented numerically in Table I.

As mentioned above this technique also yields values for the thermal conductivity, and these results are presented in Fig. 5. In addition to a gradual decrease with increasing temperature, the thermal conductivity exhibited an artifactual peak with an amplitude of 2%, at a heating power of 3 mW/cm. This peak occurred near that temperature for which the variation of the specific heat with temperature was maximum; i.e., on the high-temperature side of the specific-heat maximum. We regard this peak as an experimental effect and not indicative of the true thermal conductivity because the amplitude of the peak decreased as the heating power was decreased. The peak height was $\sim 2.0\%$ at 3 mW/cm heating power and decreased to $\sim 1.5\%$ at 1.5 mW/cm.

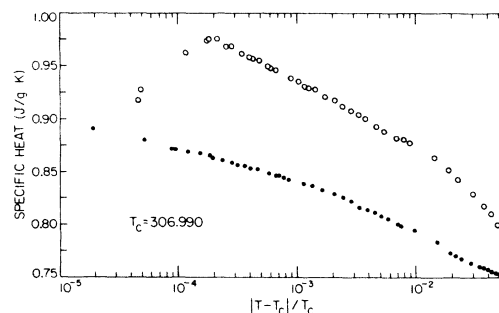


FIG. 4. Specific heat of Cr_2O_3 near the antiferromagnetic transition temperature as a function of $\log_{10}(|T - T_c|/T_c)$.

TABLE I. Specific heat of Cr_2O_3 as a function of temperature in the vicinity of the anti-ferromagnetic to paramagnetic phase transition.

T (K)	C_p ($\text{J g}^{-1} \text{K}^{-1}$)	T (K)	C_p ($\text{J g}^{-1} \text{K}^{-1}$)	T (K)	C_p ($\text{J g}^{-1} \text{K}^{-1}$)
290.678	0.7966	306.838	0.9549	307.206	0.8460
292.226	0.8030	306.855	0.9570	307.226	0.8439
293.808	0.8107	306.862	0.9585	307.251	0.8419
295.599	0.8135	306.879	0.9621	307.337	0.8378
297.773	0.8303	306.896	0.9673	307.407	0.8363
297.778	0.8301	306.903	0.9694	307.485	0.8322
300.061	0.8434	306.913	0.9688	307.619	0.8275
300.062	0.8436	306.924	0.9739	307.734	0.8247
302.643	0.8639	306.934	0.9747	307.870	0.8214
302.647	0.8630	306.936	0.9735	308.014	0.8159
304.245	0.8771	306.954	0.9627	308.178	0.8133
304.578	0.8808	306.975	0.9276	308.376	0.8112
304.901	0.8821	306.976	0.9176	308.566	0.8078
305.322	0.8891	306.996	0.8912	308.771	0.8051
305.564	0.8934	307.006	0.8797	309.156	0.7997
305.837	0.9012	307.017	0.8718	309.286	0.7985
305.985	0.9038	307.019	0.8717	309.935	0.7941
306.115	0.9088	307.027	0.8689	311.588	0.7831
306.248	0.9123	307.037	0.8675	312.923	0.7732
306.347	0.9172	307.047	0.8646	313.630	0.7711
306.458	0.9214	307.051	0.8632	314.362	0.7684
306.549	0.9278	307.063	0.8604	315.881	0.7635
306.594	0.9299	307.078	0.8583	317.535	0.7605
306.630	0.9313	307.087	0.8563	318.357	0.7596
306.668	0.9349	307.102	0.8549	319.326	0.7570
306.712	0.9390	307.115	0.8529	320.257	0.7554
306.780	0.9463	307.133	0.8521	321.253	0.7540
306.800	0.9484	307.168	0.8487	322.334	0.7530
306.811	0.9499	307.198	0.8460	323.431	0.7524

The half width of the peak was ~ 23 mK at 3 mW/cm and decreased to ~ 21 mK at 1.5 mW/cm. It is rather curious that this effect occurs in such a way as to have no noticeable effect on the measured values of the specific heat. Data from the rather narrow temperature interval over which this effect occurred were not used in the subsequent analysis, which shows this to be the transition region. There are several potential causes of such an effect, including the strong temperature dependence of the specific heat, possible nonuniformity of the transition temperature throughout the sample, a very small latent heat associated with a slight first-order transition, or inability of the sample to respond fully at the higher heating frequencies in the immediate vicinity of the transition. The possibility of detecting very small latent heats using this technique is quite promising. For example, a latent heat of only 8×10^{-4} J/cm³ would result in a distortion of the sinusoidal temperature disturbance by one percent which would be readily observable. Such a small latent heat would probably be undetectable by conventional means since it corresponds to the

amount of heat required to change the sample temperature 0.2 mK.

IV. DATA ANALYSIS

The specific-heat data have been analyzed using a nonlinear least-mean-squares fitting program, with each point weighted with an uncertainty of

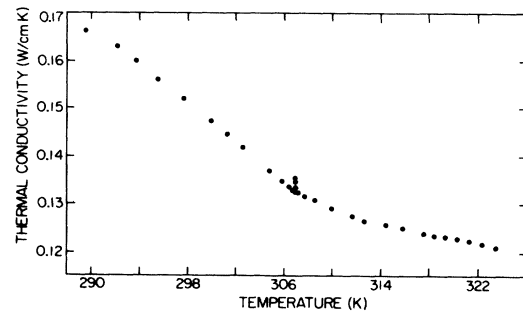


FIG. 5. Thermal conductivity of Cr_2O_3 near the anti-ferromagnetic transition temperature as a function of temperature. Peak observed at T_c is an experimental effect, and is discussed in the text.

0.1%. In carrying out this analysis we have been guided by the previous work of Kornblit and Ahlers,^{16,17} and we will employ notation similar to theirs throughout the remainder of this paper.

In its most general form the function which has been used in the analysis of specific-heat data is given by

$$C_p = (A/\alpha)|t|^{-\alpha}(1+D|t|^x) + B + Et, \quad (2)$$

where $t \equiv (T - T_c)/T_c$, and A , α , B , D , E , x , and T_c are adjustable parameters. In general those values of the parameters which result in the best fit to the data for $T > T_c$ will differ from those appropriate for $T < T_c$, and the parameters used for $T < T_c$ are denoted by being primed. This function is capable of describing cusped ($\alpha < 0$), or divergent ($\alpha > 0$) behavior, and in the limit $\alpha \rightarrow 0$ it approaches a logarithmic divergence. The dominant singularity is considered as being due to the term $A|t|^{-\alpha}$, with the factor $(1+D|t|^x)$ representing a correction to the leading power-law singularity. The term $B + Et$ is included to represent the lattice contribution and any regular contributions due to the transition itself. Rather than attempting to subtract the lattice contribution beforehand, it is important to include such a term in the actual fit so that the uncertainties in this term will be allowed for in estimating the standard deviations of the other parameters.¹⁶ The function we actually used in carrying out the fitting is

$$C_p = \tilde{A}|T - T_c|^{-\alpha}(1 + \tilde{D}|T - T_c|^x) + B + \tilde{E}(T - T_c). \quad (3)$$

This slightly different form has the advantage of reducing the correlation between sets of parameters¹⁸ such as \tilde{A} , α , and T_c ; \tilde{D} , x , and T_c , and \tilde{E} and T_c . It should be noted that this affects the standard errors for the parameters in a rather complicated way, and it is not possible to directly compare standard errors for A and \tilde{A} , D and \tilde{D} , or E and \tilde{E} . Confusion with regard to the units of the various parameters appearing in Eq. (1) can easily be avoided by regarding $T - T_c$ as actually being a dimensionless ratio, $(T - T_c)/1 \text{ K}$. Thus the units of \tilde{A} , B , and \tilde{E} are $\text{J g}^{-1} \text{K}^{-1}$, and α , \tilde{D} , and x are dimensionless.

In analyzing the specific-heat data using Eq. (3) we initially set $\tilde{D} = \tilde{D}' = 0$ and imposed the constraint $\tilde{E} = \tilde{E}'$, so that this term would be required to be regular. The additional constraint $T_c = T'_c$ resulted in no significant reduction in the quality of the fit, and consequently this constraint was also imposed for the remainder of the analysis. In order to test the extent to which the scaling law prediction $\alpha = \alpha'$ is consistent with the data, we performed the analysis using various portions of the data determined by $\tilde{t}_{\min} \leq |\tilde{t}| \leq \tilde{t}_{\max}$, where $\tilde{t} \equiv (T - T_0)/T_0$, with T_0 fixed at 306.985 K. Figure 6 shows the result-

ing values for α and α' both as functions of \tilde{t}_{\min} with \tilde{t}_{\max} fixed at 9×10^{-3} , and as functions of \tilde{t}_{\max} with \tilde{t}_{\min} fixed at 2×10^{-4} . Since α and α' were found to be equal for most of the cases analyzed, this means that these fits involve a redundant parameter. This results in poor convergence of our fitting program, and makes it difficult to estimate the standard errors. Consequently, the error bars shown are a subjective estimate based on a variety of fits. Throughout the remainder of this analysis the errors shown are one standard deviation. The results show that $\alpha = \alpha' = -0.12$ except when data very far from the transition are included. The value -0.14 is the result which has been observed in Heisenberg systems with short-range forces, and is also predicted theoretically. The fact that α and α' do not remain equal when data are included for which $\tilde{t}_{\max} > 4 \times 10^{-2}$ may indicate the need for terms of higher order than linear in describing the regular contributions, or it may be indicative of other systematic effects, as discussed below.

Since over a wide temperature range the data support $\alpha = \alpha'$, this was also incorporated as a further constraint. In order to test for possible "rounding" of the transition, or crossover from Heisenberg to Ising behavior caused by the weak anisotropy, we fixed \tilde{t}_{\max} at 9×10^{-3} and analyzed the data as a function of \tilde{t}_{\min} . The results of this analysis are presented in Table II and show no

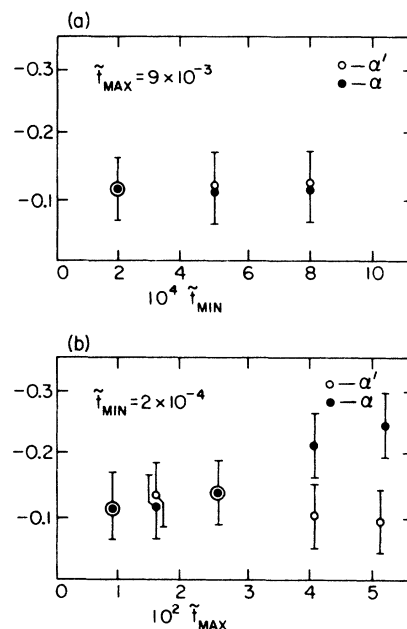


FIG. 6. (a) Exponents α and α' as a function of \tilde{t}_{\min} with \tilde{t}_{\max} fixed at 9×10^{-3} . (b) Exponents α and α' as a function of \tilde{t}_{\max} with \tilde{t}_{\min} fixed at 2×10^{-4} .

TABLE II. Values of the parameters obtained in fitting various portions of the data to Eq. (3). The constraints $\tilde{E}=\tilde{E}'$, $T_c=T_c'$, and $\alpha=\alpha'$ were employed in all cases shown, and any additional constraints imposed are indicated in each case. The rms deviation of the fit from the data is also shown in each case.

T_0 (K)	306.985	306.985	306.985	306.970
\tilde{t}_{\min}	8×10^{-4}	5×10^{-4}	2×10^{-4}	2.5×10^{-4}
\tilde{t}_{\max}	9×10^{-3}	9×10^{-3}	9×10^{-3}	9×10^{-3}
\tilde{A} ($\text{J g}^{-1} \text{K}^{-1}$)	-0.15 ± 0.04	-0.15 ± 0.02	-0.14 ± 0.01	-0.15 ± 0.01
\tilde{A}' ($\text{J g}^{-1} \text{K}^{-1}$)	-0.26 ± 0.09	-0.26 ± 0.06	-0.26 ± 0.02	-0.28 ± 0.02
α	-0.12 ± 0.03	-0.12 ± 0.02	-0.12 ± 0.01	-0.12 ± 0.01
T_c (K)	306.990 ± 0.07	306.992 ± 0.03	306.990 ± 0.006	306.983 ± 0.01
B ($\text{J g}^{-1} \text{K}^{-1}$)	0.97 ± 0.04	0.97 ± 0.02	0.97 ± 0.01	0.98 ± 0.01
B' ($\text{J g}^{-1} \text{K}^{-1}$)	1.16 ± 0.09	1.16 ± 0.06	1.16 ± 0.02	...
\tilde{E} ($\text{J g}^{-1} \text{K}^{-1}$)	-0.0033 ± 0.002	-0.0034 ± 0.001	-0.0037 ± 0.0007	-0.0033 ± 0.001
\tilde{D}	0.04 ± 0.04
\tilde{D}'	-0.71 ± 0.02
x	-0.11 ± 0.01
rms deviation	0.09%	0.08%	0.08%	0.08%
Constraints	$\tilde{D}=\tilde{D}'=0$	$\tilde{D}=\tilde{D}'=0$	$\tilde{D}=\tilde{D}'=0$	$B=B'$, $x=x'$

evidence of crossover or "rounding" for \tilde{t}_{\min} as small as 2×10^{-4} . The accuracy with which the data are fit by Eq. (3) is shown by the deviation plot of Fig. 7, which was obtained using the parameters listed in Table II with $\tilde{t}_{\min} = 2 \times 10^{-4}$ and $\tilde{t}_{\max} = 9 \times 10^{-3}$. The values of T_c obtained by these fits are very consistently equal to 306.99 K, which is the temperature for which the anomalous peak in the thermal conductivity was observed. There are three aspects of the results of this analysis which deserve further comment. First, the ratio \tilde{A}/\tilde{A}' is consistently equal to 0.56, which is quite different from the value 1.4 which is observed for Heisenberg systems,³ and the universal parameter $\mathcal{O} \equiv (1 - \tilde{A}/\tilde{A}')/\alpha$ is -3.7 , whereas other systems indicate $\mathcal{O} \cong +4$, independent of spin dimensionality.³ Second, there is a consistent indication that $B \neq B'$ which means that the specific heat is apparently discontinuous at T_c . Third, the parameter \tilde{E} is negative, while comparison with the nonmagnetic analog Al_2O_3 shows that the lattice contributions correspond to an \tilde{E} of $\sim +3 \times 10^{-3}$. This may indicate that there are significant regular contributions to the specific heat caused by the transition itself, or it could be a consequence of systematic effects such as lattice expansion.

Since the result $B \neq B'$ indicates that pure power-law behavior may not be adequate to describe the data, we reanalyzed the data in the range $2.5 \times 10^{-4} \leq |\tilde{t}| \leq 9 \times 10^{-3}$, with the additional constraints $B = B'$

and $x = x'$, but allowed \tilde{D} and \tilde{D}' to be nonzero. The results of this fit are given in Table II, as well, and must be regarded as rather peculiar. The fact that x is negative makes the correction term the leading singularity; but since $\tilde{D} \approx 0$, the behavior is still cusplike for $T > T_c$; while since $x \cong \alpha$, the behavior is nearly logarithmic for $T < T_c$. In reality, although this fit appears very different from the previous fits conceptually, it is actually almost identical to them numerically.

In order to consider the case of physically meaningful correction terms we next constrained x to lie near 0.5, which has been found satisfactory for other systems.^{3,16,17} After some difficulties in fitting we found that very good fits could be obtained using data from the range $2 \times 10^{-4} \leq |\tilde{t}|$

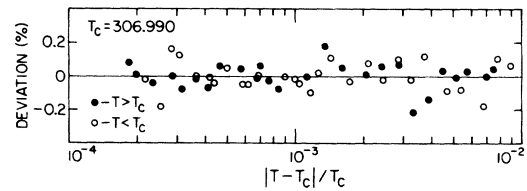


FIG. 7. Percentage deviation of the specific-heat data from the best fit to Eq. (3), with $\tilde{D}=\tilde{D}'=0$, $\alpha=\alpha'$, and $T_c=T_c'$. The analysis was carried out for $2 \times 10^{-4} \leq |\tilde{t}| \leq 9 \times 10^{-3}$ and the resulting values of the parameters are given in Table II.

$\leq 9 \times 10^{-3}$, with $T_0 = 306.96$ K, but that the quality of the fits was nearly independent of the value assigned to x , over the range $0.4 \leq x \leq 0.6$. We also noted that even with x fixed, the fitting program gave indications of redundancy in the parameters. Consequently we fixed x at 0.5 and also fixed the ratio \tilde{A}/\tilde{A}' at various values. We found that with x fixed at 0.5 we could obtain essentially perfect fits to the data (rms deviation 0.08%) irrespective of the ratio \tilde{A}/\tilde{A}' , for the entire range explored, $1.15 \leq \tilde{A}/\tilde{A}' \leq 2.05$. However, the resulting values for the universal parameter \mathcal{P} were not in agreement with results for other systems, and were only weakly dependent on \tilde{A}/\tilde{A}' , ranging from ~ 7.5 to ~ 9.5 as \tilde{A}/\tilde{A}' increased from 1.15 to 2.05. In order to be certain that no further redundancy in the parameters was involved, we fixed \tilde{A}/\tilde{A}' at 1.40, with $x = 0.5$, and began systematically decreasing α from its optimal value of -0.05 . This procedure forced the universal parameter \mathcal{P} to assume steadily decreasing values, and thus represents an inquiry into the extent to which the data can be forced to agree with the results obtained for other systems. As expected, the rms deviation increased rapidly as α was decreased, and for $\alpha = -0.09$, which results in $\mathcal{P} = 4.4$, the rms deviation was found to be 0.22%. This fit, which is presented in Table III, is statistically unacceptable. However, in light of the discussion to be presented below, the reader should bear in mind that it actually provides an

accurate description of the data. We should also like to mention one rather puzzling aspect of this analysis. Other systems rather consistently indicate $\tilde{A}/\tilde{A}' = 1.4$, while our apparently very similar data are incapable of distinguishing between values of \tilde{A}/\tilde{A}' ranging from 1.15 to 2.05.

Since the use of correction terms of the form $1 + \tilde{D}|T - T_c|^x$ did not yield results in agreement with those obtained for other systems, we returned to a pure power-law description, but imposed the additional constraint $B = B'$ so that the specific heat would be continuous at the transition. This analysis was carried out for two values of \tilde{t}_{\max} with \tilde{t}_{\min} fixed at 3×10^{-4} , and these results are also presented in Table III. Because the resulting values for T_c change somewhat when the constraint $B = B'$ is imposed, the value $T_0 = 306.915$ K was used in computing \tilde{t} . With \tilde{t}_{\max} fixed at 9×10^{-3} , the rms deviation increased to 0.15% when the constraint $B = B'$ was imposed. Again, this fit is not acceptable in a statistical sense, but does provide an excellent description of the data, although the deviations are systematic, as may be seen from the deviation plot of Fig. 8. This fit is actually very similar to that presented in the first column of Table III, because the latter resulted in very small values for \tilde{D} and \tilde{D}' . With \tilde{t}_{\max} fixed at 5.4×10^{-2} , the rms deviation is 0.28%, and again the deviations are systematic as shown in Fig. 9. Obviously this fit, which is totally unacceptable in a statistical sense, actually provides a rather ac-

TABLE III. Values of the parameters resulting from attempting to obtain fits in agreement with the results observed for Heisenberg systems.

T_0 (K)	306.957	306.915	306.915
\tilde{t}_{\min}	2×10^{-4}	3×10^{-4}	3×10^{-4}
\tilde{t}_{\max}	9×10^{-3}	9×10^{-3}	5.4×10^{-2}
\tilde{A} ($\text{J g}^{-1} \text{K}^{-1}$)	-0.34	-0.40 ± 0.06	-0.24 ± 0.02
\tilde{A}' ($\text{J g}^{-1} \text{K}^{-1}$)	-0.25 ± 0.002	-0.31 ± 0.06	-0.16 ± 0.02
α	-0.09	-0.07 ± 0.01	-0.13 ± 0.01
T_c (K)	306.921 ± 0.001	306.900 ± 0.005	306.852 ± 0.005
B ($\text{J g}^{-1} \text{K}^{-1}$)	1.15 ± 0.002	1.22 ± 0.06	1.06 ± 0.02
B' ($\text{J g}^{-1} \text{K}^{-1}$)
\tilde{E} ($\text{J g}^{-1} \text{K}^{-1}$)	$+0.0062 \pm 0.0006$	$+0.0042 \pm 0.0005$	$+0.0024 \pm 0.0001$
\tilde{D}	-0.02 ± 0.004
\tilde{D}'	-0.03 ± 0.003
x	0.50
rms deviation	0.22%	0.15%	0.28%
Constraints	$B = B', x = x',$ $\alpha = -0.09, \tilde{A}/\tilde{A}' = 1.4$	$\tilde{D} = \tilde{D}' = 0, B = B$	$\tilde{D} = \tilde{D}' = 0, B = B'$

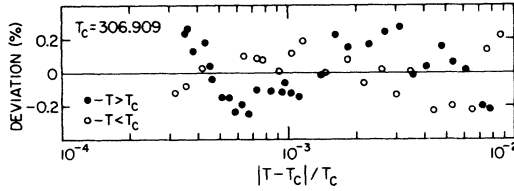


FIG. 8. Percentage deviation of the specific-heat data from the best fit to Eq. (3), with $\bar{D} = \bar{D}' = 0$, $\alpha = \alpha'$, $T_c = T'_c$, and $B = B'$. Analysis was carried out for $2 \times 10^{-4} \leq |\bar{t}| \leq 9 \times 10^{-3}$, and the resulting parameters are given in Table III.

curate description of the data over the entire temperature range studied, except for $|\bar{t}| < 2 \times 10^{-4}$ where some "rounding" is evident as was shown in Fig. 4. The results of the fits presented in Table III are in rather good agreement with the results obtained by Ahlers and Kornblit³ in their analysis of Heisenberg systems, but, of course, they do not represent optimal fits to our data.

V. DISCUSSION

The above analysis shows that if one regards the standard errors for the various parameters as reliable estimates of the actual uncertainties in the values of the parameters, then Cr_2O_3 exhibits a behavior which is neither Ising nor Heisenberg in nature, and furthermore there is no evidence of crossover from one type to the other. In reality, however, the standard deviations for the parameters only indicate the rms deviation which the best-fit value of each parameter would exhibit if the experiment were repeated many times using the same sample. The standard deviations are estimated by determining the amount by which any one parameter must be changed, *while re-optimizing all the others*, so as to result in a statistically significant increase in the value of χ^2 resulting from the fit. The actual difference between two fits which differ by an amount which is statistically significant is remarkably little. Consider, for example, the fit given in the third column of Table II. If the parameter \bar{A} is increased by *two* standard deviations, and all the other parameters are readjusted so as to optimize the new fit, the new fit and the optimal fit differ by less than 0.06% over the entire range $2 \times 10^{-4} \leq |\bar{t}| \leq 9 \times 10^{-3}$. Such a small difference can be considered significant only if one is certain that the fitting function employed is of exactly the correct form, and that there is no possibility of even very slight systematic error either in the measurements themselves or in the comparison to theory. In attempting to study critical behavior by means

of specific-heat measurements in solids this poses a particularly severe problem, not necessarily because of uncertainties in the measurements, but because the quantity measured is C_p , the specific heat at constant pressure, while the theoretical results are calculated for the case of a *rigid* lattice.¹⁹ One may estimate the magnitude of the possible differences involved using

$$C_p - C_v = T \alpha_p^2 / \rho K_T, \quad (4)$$

where $\alpha_p \equiv (1/v)(\partial v / \partial T)_p$ is the thermal-expansion coefficient and $K_T \equiv -(1/v)(\partial v / \partial p)_T$ is the isothermal compressibility. For Cr_2O_3 we may estimate α_p from the x-ray diffraction data¹⁰ as $\alpha_p \approx 5.4 \times 10^{-5} \text{ K}^{-1}$, and obtain K_T from sound speed data¹² as $K_T \approx 3.2 \times 10^{-13} \text{ cm}^2/\text{dyn}$. Equation (4) then implies that C_p and C_v differ by about 5% near T_c , and since α_p varies rather rapidly with temperature near the transition, the difference between C_p and C_v may readily change by a factor of 2. Consequently we feel that although the pure power-law fits obtained with the constraint $B = B'$ and the fit obtained using correction terms and forcing $\mathcal{P} \approx 4$, are totally unallowed in a statistical sense, it would be extremely misleading to rule them out on the basis of standard errors obtained by the fitting procedure, because they do not allow for just this sort of systematic difficulty in comparing theory and experiment. This difficulty cannot be eliminated merely by correcting C_p data so as to obtain C_v data, because the derived data for C_v would correspond to different sample volumes for each temperature, and further correction for this effect would be required. Even if this were carried out, it would be correct only for systems for which fixed volume implies a rigid lattice. This is definitely not the case with Cr_2O_3 because as the temperature increases, the c dimension expands more rapidly than the a dimension, while an increase in pressure decreases a far more than c . Since exchange constants are strongly distance dependent, the effects of lattice expansion could well result in systematic errors for

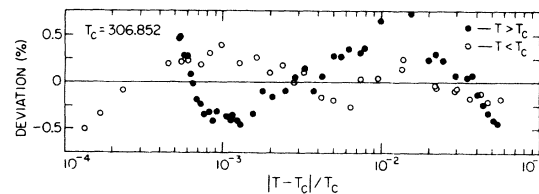


FIG. 9. Percentage deviation of the specific-heat data from the best fit to Eq. (3), with $\bar{D} = \bar{D}' = 0$, $\alpha = \alpha'$, $T_c = T'_c$, and $B = B'$. Analysis was carried out for $2 \times 10^{-4} \leq |\bar{t}| \leq 5.4 \times 10^{-2}$, and the resulting parameters are given in Table III.

many, if not all, systems. It is far from obvious that such errors can be dealt with simply by including a linear term in the fit and varying the range over which analysis is carried out. These difficulties in comparing theory and experiment are not confined to complex materials such as Cr_2O_3 . For the ideal cubic system, RbMnF_3 , C_p and C_v differ by $\sim 1.5\%$ near T_c and again the difference is quite temperature dependent. In fact, the difference between C_p and C_v will show a strong systematic dependence on $T - T_c$ for all materials because α_p behaves in a manner similar to C_p near the transition.¹⁶ In order to obtain a realistic comparison of the behavior of different materials and between experiment and theory, the magnitude and temperature dependence of possible systematic errors in the measurements must be stated, and in addition possible systematic errors in comparing the measured quantity C_p , and the theoretical results for the

rigid lattice case must also be estimated. Once this has been done, any fit which describes the data within these limits must be considered acceptable. Obviously if the existing experimental results are viewed in this light, even materials for which systematic errors are as small as a few tenths of one percent will permit vastly more latitude in the values of the various parameters than is allowed by the standard statistical errors, resulting from fits to high precision data.

ACKNOWLEDGMENTS

We are extremely grateful to Professor D. Scalapino and Professor D. Hone for many helpful discussions, to Mr. Paul Heiney for help in constructing apparatus and taking data, and to Dr. A. Narath for kindly supplying the crystal of Cr_2O_3 .

*This research supported by the National Science Foundation.

†Present address: Department of Physics, City College, Convent and 138th Streets, New York, N. Y. 10031.

¹For a discussion see L. P. Kadanoff, in *Proceedings of the International School of Physics "Enrico Fermi,"* Course LI, edited by M. S. Green (Academic, New York, 1971), p. 100.

²See K. G. Wilson and J. Kogut, *Phys. Rep. C* **12**, 75 (1974), and references therein.

³G. Ahlers and A. Kornblit, *Phys. Rev. B* **12**, 1938 (1975).

⁴P. Pfeuty, D. Jasnow, and M. E. Fisher, *Phys. Rev. B* **10**, 2088 (1974).

⁵R. E. Newnham and Y. M. de Haan, *Z. Kristallogr.* **117**, 235 (1962).

⁶L. M. Corliss, J. M. Hastings, R. Nathans, and G. Shirane, *J. Appl. Phys.* **36**, 1099 (1965).

⁷E. J. Samuelson, M. T. Hutchings, and G. Shirane, *Physica* **48**, 13 (1970).

⁸S. Foner, *Phys. Rev.* **130**, 183 (1963).

⁹J. O. Artman, J. C. Murphy, and S. Foner, *J. Appl. Phys.* **36**, 986 (1965).

¹⁰S. Greenwald, *Nature* **168**, 379 (1951).

¹¹T. Riste and A. Wanic, *Phys. Lett.* **16**, 231 (1965).

¹²A. Bachelier and C. H. Frenois, *J. Phys. (Paris)* **35**, 30 (1974).

¹³G. K. Lewis, Jr. and H. G. Drickamer, *J. Chem. Phys.* **45**, 224 (1966).

¹⁴T. G. Worlton, R. M. Brugger, and R. B. Bermion, *J. Phys. Chem. Solids* **29**, 435 (1968).

¹⁵R. H. Bruce and D. S. Cannell, *Rev. Sci. Instrum.* **47**, 1323 (1976).

¹⁶A. Kornblit and G. Ahlers, *Phys. Rev. B* **8**, 5163 (1973).

¹⁷A. Kornblit and G. Ahlers, *Phys. Rev. B* **11**, 2678 (1975).

¹⁸Use of a fitting function of the form $A|t|^{-\alpha}$ results in very strong correlation between A and α because the point $|t|=1$ lies well outside the range for which data are available, or meaningful. Thus A , which is the value assumed by the fitting function when $|t|=1$, is a quantity which is actually being determined by extrapolation from the range $|t| \lesssim 10^{-2}$, where data are available. Consequently the value obtained for A is very dependent on the value used for α . The function $\tilde{A}|T - T_c|^{-\alpha}$ does not suffer from this problem because \tilde{A} , which is the value assumed by the fitting function when $|T - T_c|=1$, is a quantity which is directly and accurately determined by the data.

¹⁹D. J. Bergman and B. I. Halperin, *Phys. Rev. B* **13**, 2145 (1976). This paper presents a detailed treatment of the behavior of an Ising system on an elastic solid of cubic or isotropic symmetry.